

8. Modeling for nonlinear analysis. An aperçu

Our objective in this chapter is to introduce some main concepts of nonlinear structural analysis. We will focus on the fundamental issues.

We choose the analysis of truss structures as a means to discuss in a simple setting the basic concepts of nonlinear analysis. Let us recall that in Chapter 2 truss structures were used to exemplify the application of the fundamental steps in structural mechanics leading to the matrix formulation. Later, several more complex mathematical models and finite element formulations were presented. Despite the complexity of these models, we could always find a clear analogy between their formulations and those for truss structures.

Of course, it is out of the scope of this book to discuss nonlinear formulations for the 2-D, 3-D, beam and shell mathematical models detailed in Chapters 3 and 4 (for such formulations see Bathe, 1996). However, we do endeavour to make the presentation for truss structures sufficiently comprehensive for the reader to gain insight into the important general aspects of nonlinear analysis of complex problems. In our presentation we use the notation of Bathe, 1996.

8.1 Sources of nonlinearity

We can classify many nonlinearities encountered in structural analysis as geometric, material and contact nonlinearities (see Bathe, 1996). Of course, in a general nonlinear analysis, these nonlinearities may arise together. We give below an introductory discussion of these nonlinearities.

Geometric nonlinearities

A most important assumption of linear analysis – introduced in Chapter 2 – is that the displacements are assumed to be infinitesimally small. This assumption is adequate for most applications of structural engineering. However, there are situations in which it does not apply. Consider, for example, the trusses described in Figure 8.1.

The truss of Figure 8.1a corresponds to the truss defined in Figure 2.16 with $R_1 = R_2 = -\frac{R\sqrt{2}}{2}$ and the cross-sectional areas $A = A_1 = A_2 =$

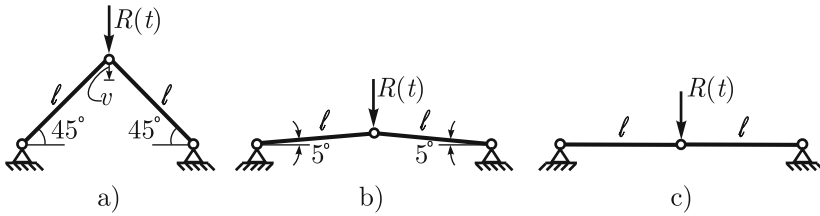


Fig. 8.1. Selected truss structures ($\ell = 2 \text{ m}$)

$1.5 \times 10^{-3} \text{ m}$. The displacement v under the load can be readily evaluated considering linear analysis and is given by

$$v = \frac{R\ell}{2EA \sin(45^\circ)^2} = 0.000508 \text{ m}$$

which is very small compared to the dimensions of the truss. Therefore, the linear assumption – imposing equilibrium in the undeformed configuration – is adequate. For the truss of Figure 8.1b the linear analysis leads to

$$v = \frac{R\ell}{2EA \sin(5^\circ)^2} = 0.033434 \text{ m}$$

which is a somewhat large value when compared to the height $H = \ell \sin 5^\circ = 0.17431 \text{ m}$ and, hence, imposing the equilibrium in the undeformed configuration might not be an appropriate assumption.

In order to solve the problem allowing for any magnitude of displacement we need to guarantee that equilibrium is satisfied in the deformed configuration which is not known a priori. We solve this problem in Example 8.1 below and valuable insight in the nonlinear formulation will be gained from this solution.

Finally, we note that the truss of Figure 8.1c can display infinitesimally small rigid motions and therefore can not be solved in linear analysis.

In nonlinear analysis, it is usual to consider that the load is increased from zero to a given value. We can describe such load variation by a function

$${}^t R = R(t)$$

where t is the time variable. Since we pursue a static analysis the loads are assumed to be applied slowly, so that inertia effects are negligible. Therefore, the time variable is merely used to define how the load varies during the analysis. The nonlinear solution will then give the deformed configuration for every time t in the range of interest. Of course, equilibrium will be enforced in these deformed configurations.

Example 8.1¹

Consider the arch described in Figure 8.2a which can be modeled as a one bar truss structure. Obtain the deformed configurations associated with tR

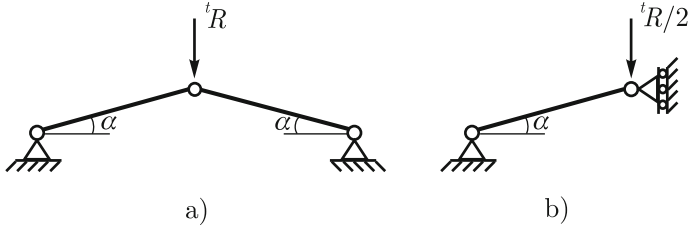


Fig. 8.2. a) Arch structure; b) Model using symmetry

which is increased from zero. Assume that α is small such that the resulting strain is also small and, therefore, Hooke’s law applies.

Solution

The kinematics of the structure is summarized in Figure 8.3a from which we can write

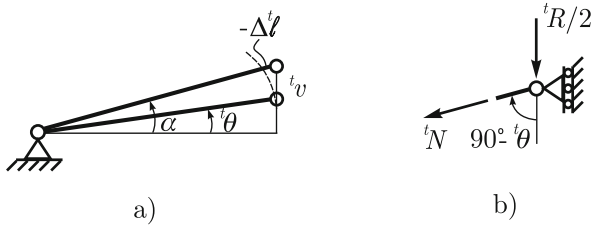


Fig. 8.3. a) Kinematics of the truss; b) Normal force for a deformed configuration

$${}^0l = l, \quad \Delta{}^t l = {}^t l - {}^0 l$$

$${}^t l \cos {}^t \theta = {}^0 l \cos \alpha$$

$${}^t l \sin {}^t \theta = {}^0 l \sin \alpha - {}^t v$$

which yields

¹ This example is also discussed in (Bathe, 1996, Example 6.3)

$$\Delta^t \ell = \sqrt{({}^0 \ell)^2 - 2 {}^0 \ell {}^t v \sin \alpha + ({}^t v)^2} - {}^0 \ell \quad (8.1)$$

and

$$\sin {}^t \theta = \frac{{}^0 \ell \sin \alpha - {}^t v}{{}^0 \ell + \Delta^t \ell}. \quad (8.2)$$

Referring to Figure 8.3b, equilibrium gives

$$\frac{{}^t R}{2} = - {}^t N \sin {}^t \theta \quad (8.3)$$

where ${}^t N$ is the axial force of the bar at time t . Since the strains are small we can use Hooke's law to obtain

$${}^t N = EA \frac{\Delta^t \ell}{{}^0 \ell}. \quad (8.4)$$

From equations (8.1), (8.2), (8.3) and (8.4), we obtain

$$\frac{{}^t R}{2EA} = \left(\frac{1}{\sqrt{1 - 2 \frac{{}^t v}{{}^0 \ell} \sin \alpha + \left(\frac{{}^t v}{{}^0 \ell}\right)^2}} - 1 \right) \left(\sin \alpha - \frac{{}^t v}{{}^0 \ell} \right). \quad (8.5)$$

We note that equation (8.5) allows to obtain the deformed configurations in which ${}^t R$ is in equilibrium with the bar forces in the deformed configurations.

In Figure 8.4a the load-displacement relation is given when $\alpha = 5^\circ$. We note that for small ${}^t R$ the response is almost linear (up to point C). For the load level between points C and A the response is truly nonlinear. At the configuration corresponding to point A , with a “tiny” load increase the structure “snaps” and reaches an equilibrated² configuration corresponding to point B . The configurations corresponding to points A and B are schematically presented in Figure 8.4b and, although the load increase was “tiny”, the structure could not reach an equilibrated configuration in the vicinity of the configuration corresponding to point A . The configurations between those of points A and B can only be reached by imposing displacements. The load level R_{cr} corresponding to the *limit point* A is called the *critical load*.

□

Material nonlinearities

The discussion presented so far assumed that the material has a linear elastic behavior. However, there are situations for which the use of a nonlinear material behavior is essential for correct modeling. Nonlinear elastic and elasto-plastic behaviors are common examples.

² Since the structural motion corresponding to the “snap” occurs in a short time period, in physical reality, the structure would oscillate around the configuration given by point B , before this configuration is finally reached due to energy dissipation

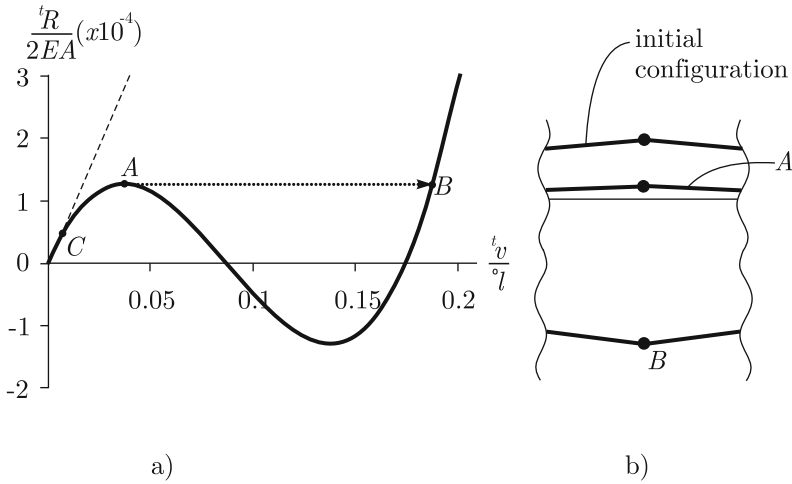


Fig. 8.4. a) Load-displacement curve. Linear response shown by the dashed line; b) Selected configurations around middle node

In the discussion below we address only one-dimensional states of stress and strain which are those relevant to the truss formulation and which allow us to introduce the main concepts.

We recall the linear elastic behavior in Figure 8.5a and introduce the nonlinear elastic behavior in Figure 8.5b. The essential ingredient of an elastic behavior is that the deformations are immediate and reversible. The deformation being immediate means that there is no time lag between the development of a strain state given a stress state. The reversibility means that the stress state depends only on the current strain state, *i.e.*, not on any history of stress and strain. For example, for point A shown on the diagrams of Figure 8.5, loading and unloading may have occurred many times before the stress and strain states associated with A have been reached.

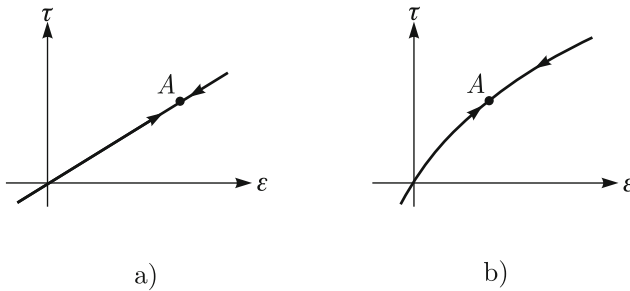


Fig. 8.5. a) Linear elastic; b) Nonlinear elastic

Let us consider an elasto-plastic behavior as an example in which inelastic deformations take place. In Figure 8.6a typical test data from a uniaxial tension laboratory experiment of a metallic material is presented. The arrows indicate the loading and unloading paths. We note the strongly nonlinear behavior and that upon unloading a residual strain ε^p – the plastic strain – is present. In Figure 8.6b a model representation of the data of Figure 8.6a is shown. In this bilinear model the behavior is purely elastic until the yield stress τ_y is reached at point 1. Above this stress level, the increments in stress and strain are related by the modulus E_T (hardening modulus) and unloading, like from point 2, occurs according to the Young's modulus E of the material. Total unloading will lead to a residual plastic deformation ε^p . Reloading from this point (point 3), the behavior is purely elastic up to point 4, indicating that the yield stress has increased (strain hardening), and then loading continues like to point 5.

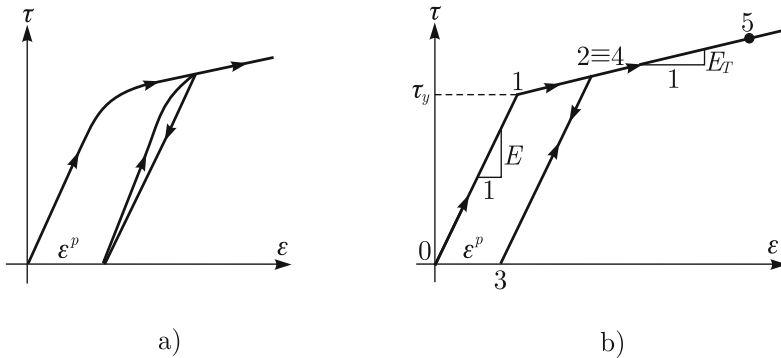


Fig. 8.6. a) Stress-strain response from a laboratory experiment; b) Model stress-strain curve

If we assume $E_T = 0$ there is no strain hardening and the material is referred to as elastic perfectly plastic.

Of course, the modeling of plasticity is a very large field in solid mechanics (see *e.g.* Kojic and Bathe, 2005) but the behavior mentioned above already allows us to present a valuable analysis example.

Example 8.2

Evaluate the load displacement response of the truss of Figure 8.7a; increase the load P from zero up to start of collapse of the structure and then totally unload the structure. The material is elastic perfectly plastic as described in Figure 8.7b.

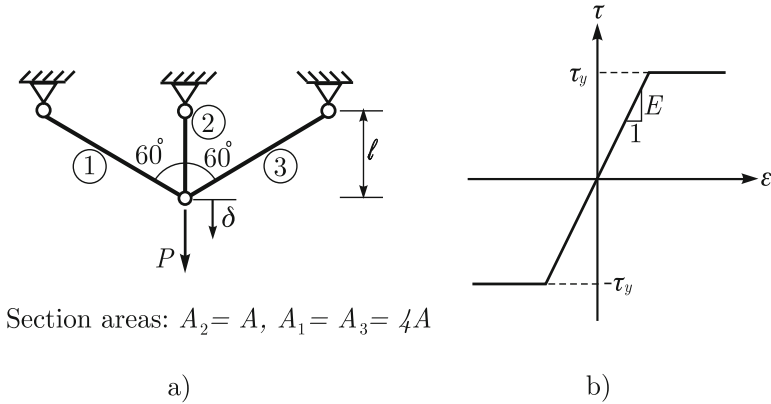


Fig. 8.7. a) Truss structure; b) Stress-strain curve adopted

Solution

We suppose that the displacements are small enough such that equilibrium is appropriately enforced in the undeformed configuration, and the nonlinear behavior is due only to the material behavior. We refer to such analyses as materially–nonlinear–only (M.N.O.) analyses.

The initial response of the structure is elastic. Due to symmetry conditions $N_1 = N_3$ and equilibrium yields

$$2N_1 \cos 60^\circ + N_2 = P \quad \Rightarrow \quad N_1 + N_2 = P.$$

Referring to Figure 8.8, compatibility yields

$$\Delta \ell_2 = 2\Delta \ell_1$$

and since

$$\Delta \ell_1 = \frac{N_1 \ell_1}{E_1 A_1} = \frac{N_1 \ell}{2EA} \quad \text{and} \quad \Delta \ell_2 = \frac{N_2 \ell_2}{E_2 A_2} = \frac{N_2 \ell}{EA}$$

we obtain

$$N_1 = N_2 = \frac{P}{2}.$$

During the elastic phase, the stresses in the bars are given by

$$\tau_1 = \frac{P}{2A_1} = \frac{P}{8A} \quad \text{and} \quad \tau_2 = \frac{P}{2A_2} = \frac{P}{2A}.$$

Therefore, bar 2 attains its plastic limit first at the load P_I which is given by

$$P_I = 2\tau_y A$$

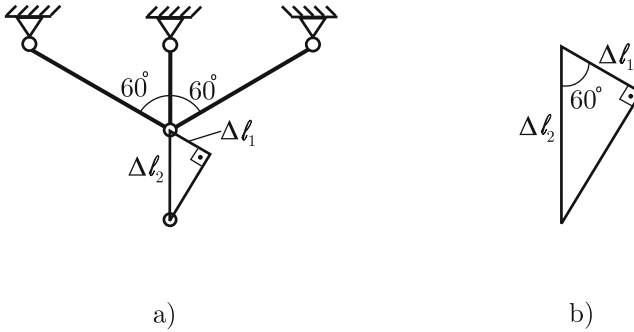


Fig. 8.8. a) Compatibility of displacements; b) Geometric relations

and the stress at bar 1 for this load is

$$\tau_1 = \frac{P_I}{2A_1} = \frac{\tau_y}{4}.$$

For increments of load beyond P_I , only bars 1 and 3 have stiffness and bar 2 will deform, without increase in stress, to maintain compatibility. From equilibrium

$$2\Delta N_1 \cos 60^\circ = \Delta P \quad \Rightarrow \quad \Delta N_1 = \Delta P.$$

The collapse of the structure is attained when the stress in bars 1 and 3 is equal to τ_y . Then the structure is no longer able to sustain load increments. Therefore, the load P_{II} at the collapse of the structure is given by

$$P_{II} = P_I + \Delta P^{II}$$

where

$$\frac{\Delta P^{II}}{4A} + \frac{\tau_y}{4} = \tau_y$$

leading to

$$P_{II} = 5\tau_y A.$$

The unloading is initially elastic for all three bars. However, bar 2 might attain its compression yield stress before total unloading. In fact, the total unloading requires

$$\Delta P = -5\tau_y A$$

leading to

$$\Delta\tau_2 = \frac{\Delta N_2}{A} = \frac{\Delta P}{2A} < -2\tau_y$$

Therefore, the elastic part of the unloading phase associated with ΔP^e can be evaluated by imposing

$$\Delta\tau_2 = \frac{\Delta N_2}{A} = \frac{\Delta P^e}{2A} = -2\tau_y$$

leading to

$$\Delta P^e = -4\tau_y A.$$

For the final unloading phase only bars 1 and 3 change stress.

Since bars 1 and 3 remain elastic throughout the loading and unloading phases they characterize the truss deformation. We note that

$$\delta = \Delta\ell_2 = 2\Delta\ell_1 = \frac{N_1\ell}{2EA}.$$

Let point A be associated with the yielding of bar 2 in tension; point B with

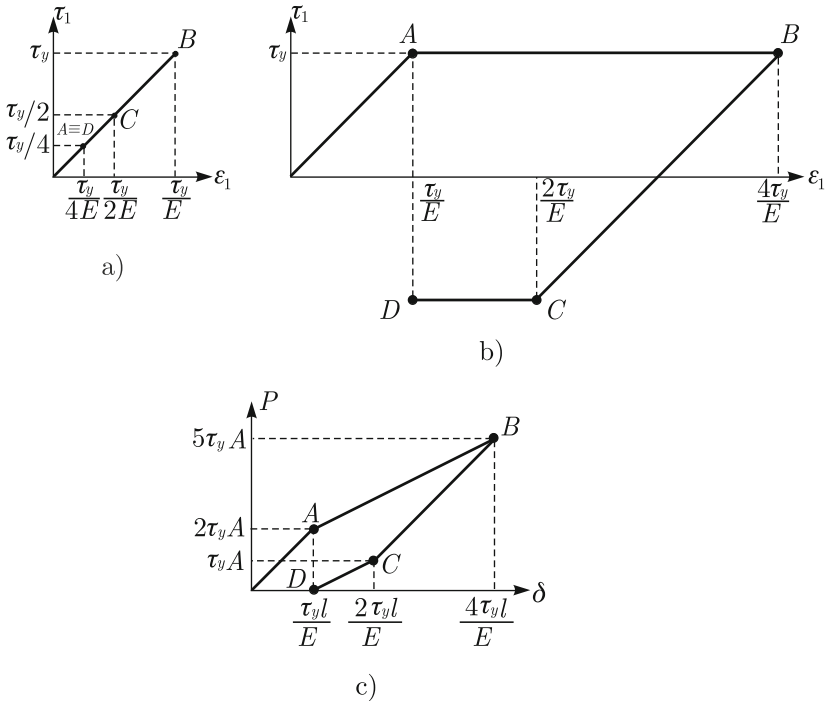


Fig. 8.9. a) Response of bars 1 and 3; b) Response of bar 2; c) Response of the structure

the imminence of collapse; point C with the yielding of bar 2 in compression

and point D with total unloading. Then, Figure 8.9 summarizes the response of the structure.

We should note the path dependency of the response of the structure and that at the final configuration, without any external load, bars 1 and 3 are in tension and bar 2 is in compression, all with residual stresses.

□

Contact nonlinearities

Contact nonlinearities arise when during the deformation process a body establishes contact with other bodies or with itself. In essence, contact conditions correspond to a change of boundary conditions on the body coming into contact. A typical situation for a simple truss is presented in Figure 8.10.

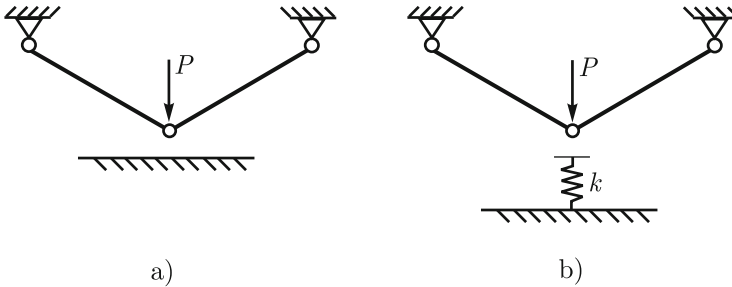


Fig. 8.10. a) Contact implying a change of boundary condition; b) Spring modeling the contact

Other sources of nonlinearities

In addition to the common sources of nonlinearities mentioned above, there are other instances. For example, during construction or manufacturing processes, structural parts may be added or suppressed which affect the subsequent structural response. Also, problems with fluid-structure interactions and thermo-mechanical interactions lead in general to a nonlinear response, see *e.g.* Bathe, 2005.

8.2 Incremental formulation for nonlinear analysis

A basic result of the matrix analysis of truss structures derived in Chapter 2 was that for a given \mathbf{R} , the column matrix of external nodal loads, the equilibrium conditions are given by

$$\mathbf{F} = \mathbf{R}$$

where \mathbf{F} is column matrix of the nodal forces corresponding to the element stresses. We also call these nodal point forces corresponding to the element stresses, internal nodal point forces. In linear analysis, introducing the compatibility conditions and constitutive behaviors, we obtain

$$\mathbf{F} = \mathbf{KU} \quad (8.6)$$

which leads to the final matrix equation

$$\mathbf{KU} = \mathbf{R}.$$

In nonlinear analysis equation (8.6) is no longer valid since the nodal forces \mathbf{F} depend nonlinearly on the nodal displacements.

Let us assume that the external nodal loads do not depend on the nodal displacements and are given by ${}^t\mathbf{R}$ where t is the time variable representing the load and the configuration at time t .

The equilibrium conditions at time t can be expressed as

$${}^t\mathbf{F} = {}^t\mathbf{R} \quad (8.7)$$

where ${}^t\mathbf{F}$ are the nodal forces corresponding to the element stresses for the configuration at time t , *i.e.*,

$${}^tF_i = {}^tF_i({}^tU_1, {}^tU_2, \dots, {}^tU_N) \quad \text{for } i = 1, \dots, N \quad (8.8)$$

which in matrix notation is given by

$${}^t\mathbf{F} = {}^t\mathbf{F}({}^t\mathbf{U}) \quad (8.9)$$

where

$${}^t\mathbf{U}^T = \left[{}^tU_1 \quad {}^tU_2 \quad \dots \quad {}^tU_N \right]$$

gives the nodal displacements at time t . In a nonlinear problem, the tF_i of equation (8.8) depend nonlinearly on tU_j , $j = 1, \dots, N$. Therefore, to solve directly (8.7) is, in general not possible. This fact prompts us to introduce the incremental procedure as an effective approach to solve (8.7).

The fundamental idea of the incremental procedure is to suppose that the solution is known at time t and develop a methodology to obtain the solution at time $t + \Delta t$, where Δt is a finite time increment referred to as “the time step” corresponding to positive or negative “increments” in forces and displacements. With this methodology available, we can obtain, starting from time $t = 0$, the solution for any time t by applying repeatedly this time-step solution scheme (see also Bathe, 1996).

We may write

$${}^{t+\Delta t}\mathbf{F} = {}^t\mathbf{F} + \mathbf{F} \quad (8.10)$$

where \mathbf{F} is the unknown internal nodal force increment such that

$${}^{t+\Delta t}\mathbf{F} = {}^{t+\Delta t}\mathbf{R}. \quad (8.11)$$

Substituting (8.10) into (8.11) yields

$$\mathbf{F} = {}^{t+\Delta t}\mathbf{R} - {}^t\mathbf{F}. \quad (8.12)$$

Let dF_i be an infinitesimally small internal nodal force increment for degree of freedom i which is given by

$$dF_i = \sum_{j=1}^N \frac{\partial {}^tF_i}{\partial {}^tU_j} dU_j \quad (8.13)$$

where the dU_j are infinitesimally small nodal displacement increments. Defining

$${}^t\mathbf{K} = \begin{bmatrix} \frac{\partial {}^tF_1}{\partial {}^tU_1} & \frac{\partial {}^tF_1}{\partial {}^tU_2} & \cdots & \frac{\partial {}^tF_1}{\partial {}^tU_N} \\ \vdots & \ddots & & \vdots \\ \vdots & & \ddots & \vdots \\ \frac{\partial {}^tF_N}{\partial {}^tU_1} & \cdots & \cdots & \frac{\partial {}^tF_N}{\partial {}^tU_N} \end{bmatrix} \quad (8.14)$$

we can re-write (8.13) as

$$d\mathbf{F} = {}^t\mathbf{K} d\mathbf{U} \quad (8.15)$$

where the $d\mathbf{F}$ and $d\mathbf{U}$ are column matrices which collect the increments dF_i , dU_j defined above. The matrix ${}^t\mathbf{K}$ defined by equation (8.14) is called the tangent stiffness matrix at time t with the obvious interpretation given by (8.15) that it relates the infinitesimally small increments of nodal displacements to the infinitesimally small increments of internal nodal point forces.

Let us define, considering equation (8.12), a first estimate $\Delta\mathbf{U}^{(1)}$ for the increment of nodal displacements from time t to time $t + \Delta t$ by

$${}^t\mathbf{K} \Delta\mathbf{U}^{(1)} = {}^{t+\Delta t}\mathbf{R} - {}^t\mathbf{F} \quad (8.16)$$

where we naturally use (8.15), but for larger and complex load changes. We note that the right hand side of equation (8.16) is the out-of-balance load when we change the external load from ${}^t\mathbf{R}$ to ${}^{t+\Delta t}\mathbf{R}$. The column matrix $\Delta\mathbf{U}^{(1)}$ is, in general, only an approximation of the exact nodal displacement increment. A first estimate of the nodal displacements at time $t + \Delta t$ is therefore given by

$${}^{t+\Delta t}\mathbf{U}^{(1)} = {}^t\mathbf{U} + \Delta\mathbf{U}^{(1)}$$

and

$${}^{t+\Delta t}\mathbf{F}^{(1)} = {}^{t+\Delta t}\mathbf{F} \left({}^{t+\Delta t}\mathbf{U}^{(1)} \right)$$

defines the internal nodal point forces corresponding to the nodal displacements ${}^{t+\Delta t}\mathbf{U}^{(1)}$. We can evaluate the out-of-balance load ${}^{t+\Delta t}\mathbf{R} - {}^{t+\Delta t}\mathbf{F}^{(1)}$ associated with the intermediate configuration (between t and $t + \Delta t$) given by ${}^{t+\Delta t}\mathbf{U}^{(1)}$, and then obtain a second nodal displacement increment $\Delta\mathbf{U}^{(2)}$ from

$${}^{t+\Delta t}\mathbf{K}^{(1)} \Delta\mathbf{U}^{(2)} = {}^{t+\Delta t}\mathbf{R} - {}^{t+\Delta t}\mathbf{F}^{(1)}.$$

Hence we obtain

$${}^{t+\Delta t}\mathbf{U}^{(2)} = {}^{t+\Delta t}\mathbf{U}^{(1)} + \Delta\mathbf{U}^{(2)}$$

and

$${}^{t+\Delta t}\mathbf{F}^{(2)} = {}^{t+\Delta t}\mathbf{F} \left({}^{t+\Delta t}\mathbf{U}^{(2)} \right).$$

Note that ${}^{t+\Delta t}\mathbf{K}^{(1)}$ is the tangent stiffness matrix for the intermediate configuration given by ${}^{t+\Delta t}\mathbf{U}^{(1)}$, *i.e.*,

$${}^{t+\Delta t}K_{ij}^{(1)} = \left. \frac{\partial {}^{t+\Delta t}F_i}{\partial {}^{t+\Delta t}U_j} \right|_{{}^{t+\Delta t}\mathbf{U}^{(1)}}.$$

This iterative procedure is repeated until the out-of-balance load ${}^{t+\Delta t}\mathbf{R} - {}^{t+\Delta t}\mathbf{F}^{(k)}$ is sufficiently small. We refer the reader to Bathe, 1996 for more details and a discussion of the convergence of the iteration. When we have found ${}^{t+\Delta t}\mathbf{U}^{(k)}$ for which convergence has been achieved, we set

$${}^{t+\Delta t}\mathbf{U} = {}^{t+\Delta t}\mathbf{U}^{(k)}$$

and the next time step is considered.

The iteration procedure for each time step can be summarized by

$$\begin{aligned} {}^{t+\Delta t}\mathbf{K}^{(i-1)} \Delta\mathbf{U}^{(i)} &= {}^{t+\Delta t}\mathbf{R} - {}^{t+\Delta t}\mathbf{F}^{(i-1)} \\ {}^{t+\Delta t}\mathbf{U}^{(i)} &= {}^{t+\Delta t}\mathbf{U}^{(i-1)} + \Delta\mathbf{U}^{(i)} \end{aligned}$$

with the initial conditions

$${}^{t+\Delta t}\mathbf{U}^{(0)} = {}^t\mathbf{U}, \quad {}^{t+\Delta t}\mathbf{K}^{(0)} = {}^t\mathbf{K}, \quad {}^{t+\Delta t}\mathbf{F}^{(0)} = {}^t\mathbf{F}.$$

The tangent stiffness matrix is a fundamental ingredient for the incremental procedure and hence we need to address how to obtain ${}^t\mathbf{K}$ for a truss structure. As in linear analysis, we obtain ${}^t\mathbf{K}$ by summing up the stiffness

contributions of the truss elements of the assemblage. Therefore, if we have the tangent stiffness matrix ${}^t\mathbf{k}$ for a generic truss element, we can obtain ${}^t\mathbf{K}$ as in linear analysis (see Section 2.3).

Nonlinear stiffness matrix of a truss element

We follow in this derivation Example 6.16 of Bathe, 1996 and consider the configurations at time 0 and t of a generic truss element as summarized in Figure 8.11a. For simplicity of the derivations and interpretations, the truss

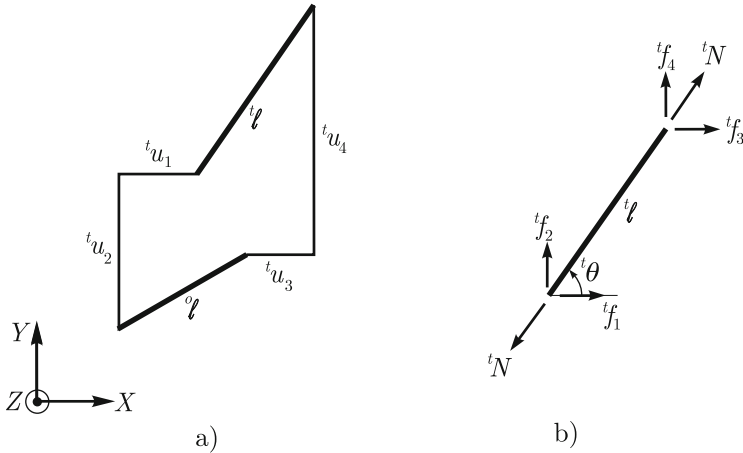


Fig. 8.11. a) Nodal displacement for a truss element; b) Nodal forces for a truss element

element is supposed to be in the XY plane throughout the motion. In Figure 8.11a we show the nodal displacements for time t and in Figure 8.11b the nodal forces where we also show the axial force tN and the angle ${}^t\theta$ that the bar axis makes with respect to the global X axis, both for time t .

The generic term of the tangent stiffness matrix of the truss element at time t is given by

$${}^tk_{ij} = \frac{\partial {}^tf_i}{\partial {}^tu_j}.$$

The column matrix of nodal displacements and nodal forces at time t are given by

$${}^t\mathbf{u} = \begin{bmatrix} {}^tu_1 \\ {}^tu_2 \\ {}^tu_3 \\ {}^tu_4 \end{bmatrix}, \quad {}^t\mathbf{f} = \begin{bmatrix} {}^tf_1 \\ {}^tf_2 \\ {}^tf_3 \\ {}^tf_4 \end{bmatrix}.$$

Referring to Figure 8.11b, we can write

$${}^t\mathbf{f} = \begin{bmatrix} - {}^tN \cos {}^t\theta \\ - {}^tN \sin {}^t\theta \\ {}^tN \cos {}^t\theta \\ {}^tN \sin {}^t\theta \end{bmatrix}. \tag{8.17}$$

Therefore, to evaluate ${}^t\mathbf{k}$ we need to calculate the derivatives of tN and ${}^t\theta$ with respect to the nodal displacements tu_i . Referring to Figure 8.12, we

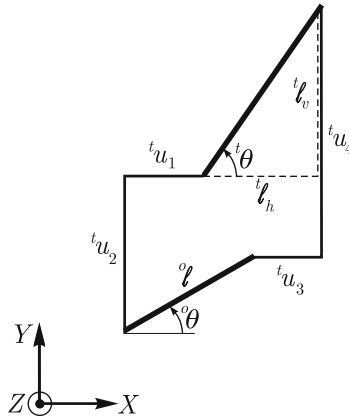


Fig. 8.12. Additional definitions related to the truss element kinematics

define the horizontal and vertical projections of the bar length at time t by

$${}^t\ell_h = {}^t\ell \cos {}^t\theta = {}^0\ell \cos {}^0\theta + {}^tu_3 - {}^tu_1 \tag{8.18}$$

$${}^t\ell_v = {}^t\ell \sin {}^t\theta = {}^0\ell \sin {}^0\theta + {}^tu_4 - {}^tu_2 \tag{8.19}$$

and defining

$${}^t\ell = {}^0\ell + \Delta^t\ell$$

we can re-write (8.18) and (8.19) as

$${}^t\ell_h = ({}^0\ell + \Delta^t\ell) \cos {}^t\theta \tag{8.20}$$

$${}^t\ell_v = ({}^0\ell + \Delta^t\ell) \sin {}^t\theta. \tag{8.21}$$

A generic element of ${}^t\mathbf{k}$ can be written as

$${}^tk_{ij} = \frac{\partial {}^tf_i}{\partial {}^tu_j} = \frac{\partial {}^tf_i}{\partial {}^t\ell_h} \frac{\partial {}^t\ell_h}{\partial {}^tu_j} + \frac{\partial {}^tf_i}{\partial {}^t\ell_v} \frac{\partial {}^t\ell_v}{\partial {}^tu_j}. \tag{8.22}$$

Note that we can easily obtain $\frac{\partial {}^t\ell_h}{\partial {}^tu_j}$ and $\frac{\partial {}^t\ell_v}{\partial {}^tu_j}$ from equations (8.18) and (8.19). Therefore, let us focus on the terms $\frac{\partial {}^tf_i}{\partial {}^t\ell_h}$ and $\frac{\partial {}^tf_i}{\partial {}^t\ell_v}$.

From equations (8.20) and (8.21), we obtain

$$\begin{bmatrix} \frac{\partial}{\partial(\Delta^t\ell)} \\ \frac{\partial}{\partial {}^t\theta} \end{bmatrix} = \begin{bmatrix} \cos {}^t\theta & \sin {}^t\theta \\ -({}^0\ell + \Delta^t\ell) \sin {}^t\theta & ({}^0\ell + \Delta^t\ell) \cos {}^t\theta \end{bmatrix} \begin{bmatrix} \frac{\partial}{\partial {}^t\ell_h} \\ \frac{\partial}{\partial {}^t\ell_v} \end{bmatrix}$$

which upon inversion leads to

$$\begin{bmatrix} \frac{\partial}{\partial {}^t\ell_h} \\ \frac{\partial}{\partial {}^t\ell_v} \end{bmatrix} = \begin{bmatrix} \cos {}^t\theta & -\frac{\sin {}^t\theta}{{}^0\ell + \Delta^t\ell} \\ \sin {}^t\theta & \frac{\cos {}^t\theta}{{}^0\ell + \Delta^t\ell} \end{bmatrix} \begin{bmatrix} \frac{\partial}{\partial(\Delta^t\ell)} \\ \frac{\partial}{\partial {}^t\theta} \end{bmatrix}.$$

Therefore,

$$\begin{bmatrix} \frac{\partial {}^tf_i}{\partial {}^t\ell_h} \\ \frac{\partial {}^tf_i}{\partial {}^t\ell_v} \end{bmatrix} = \begin{bmatrix} \cos {}^t\theta & -\frac{\sin {}^t\theta}{{}^0\ell + \Delta^t\ell} \\ \sin {}^t\theta & \frac{\cos {}^t\theta}{{}^0\ell + \Delta^t\ell} \end{bmatrix} \begin{bmatrix} \frac{\partial {}^tf_i}{\partial(\Delta^t\ell)} \\ \frac{\partial {}^tf_i}{\partial {}^t\theta} \end{bmatrix} \tag{8.23}$$

together with equation (8.22) give us the element of tk .

Let us detail the evaluation of one term. For example, to obtain ${}^tk_{11}$ we need

$$\begin{aligned} \frac{\partial {}^tf_1}{\partial \Delta^t\ell} &= -\frac{\partial {}^tN}{\partial \Delta^t\ell} \cos {}^t\theta, & \frac{\partial {}^tf_1}{\partial {}^t\theta} &= {}^tN \sin {}^t\theta \\ \frac{\partial {}^t\ell_h}{\partial {}^tu_1} &= -1, & \frac{\partial {}^t\ell_v}{\partial {}^tu_1} &= 0. \end{aligned}$$

Using the above relations together with (8.23) and (8.22), we obtain

$$k_{11} = \frac{\partial {}^tN}{\partial \Delta^t\ell} \cos^2 {}^t\theta + \frac{{}^tN}{{}^0\ell + \Delta^t\ell} \sin^2 {}^t\theta. \tag{8.24}$$

This equation can be written in an alternative form using the derivative rule of the quotient of functions

$$\frac{\partial {}^tN}{\partial \Delta^t\ell} = \frac{\partial}{\partial \Delta^t\ell} \left(\frac{{}^tN}{{}^0\ell + \Delta^t\ell} \right) ({}^0\ell + \Delta^t\ell) + \frac{{}^tN}{{}^0\ell + \Delta^t\ell}$$

which substituted in (8.24) yields

$$k_{11} = \frac{\partial}{\partial \Delta^t\ell} \left(\frac{{}^tN}{{}^0\ell + \Delta^t\ell} \right) ({}^0\ell + \Delta^t\ell) \cos^2 {}^t\theta + \frac{{}^tN}{{}^0\ell + \Delta^t\ell}.$$

The other terms of the stiffness matrix can be obtained analogously leading to

$$\begin{aligned}
 {}^t\mathbf{k} &= \frac{\partial}{\partial \Delta^t\ell} \left(\frac{{}^tN}{{}^0\ell + \Delta^t\ell} \right) ({}^0\ell + \Delta^t\ell) \\
 &\left[\begin{array}{cccc}
 \cos^2 {}^t\theta & \sin {}^t\theta \cos {}^t\theta & -\cos^2 {}^t\theta & -\sin {}^t\theta \cos {}^t\theta \\
 \sin {}^t\theta \cos {}^t\theta & \sin^2 {}^t\theta & -\sin {}^t\theta \cos {}^t\theta & -\sin^2 {}^t\theta \\
 -\cos^2 {}^t\theta & -\sin {}^t\theta \cos {}^t\theta & \cos^2 {}^t\theta & \sin {}^t\theta \cos {}^t\theta \\
 -\sin {}^t\theta \cos {}^t\theta & -\sin^2 {}^t\theta & \sin {}^t\theta \cos {}^t\theta & \sin^2 {}^t\theta
 \end{array} \right] \\
 &+ \frac{{}^tN}{{}^0\ell + \Delta^t\ell} \left[\begin{array}{cccc}
 1 & 0 & -1 & 0 \\
 0 & 1 & 0 & -1 \\
 -1 & 0 & 1 & 0 \\
 0 & -1 & 0 & 1
 \end{array} \right] = {}^t\mathbf{k}_L + {}^t\mathbf{k}_{NL}
 \end{aligned} \tag{8.25}$$

where we partitioned ${}^t\mathbf{k}$ into ${}^t\mathbf{k}_L$, the linear part, and ${}^t\mathbf{k}_{NL}$, the nonlinear part of the tangent stiffness matrix (see also (8.26)).

Let us now assume that the displacements are large but the strains are small, and that Hooke's law applies. Then

$${}^tN = \frac{EA}{{}^0\ell} \Delta^t\ell.$$

Note that, for such case,

$$\frac{\partial}{\partial \Delta^t\ell} \left(\frac{{}^tN}{{}^0\ell + \Delta^t\ell} \right) ({}^0\ell + \Delta^t\ell) = \frac{EA}{{}^0\ell + \Delta^t\ell}$$

which substituted in equation (8.25) gives

$$\begin{aligned}
 {}^t\mathbf{k} &= \frac{EA}{{}^0\ell + \Delta^t\ell} \left[\begin{array}{cccc}
 \cos^2 {}^t\theta & \sin {}^t\theta \cos {}^t\theta & -\cos^2 {}^t\theta & -\sin {}^t\theta \cos {}^t\theta \\
 \sin {}^t\theta \cos {}^t\theta & \sin^2 {}^t\theta & -\sin {}^t\theta \cos {}^t\theta & -\sin^2 {}^t\theta \\
 -\cos^2 {}^t\theta & -\sin {}^t\theta \cos {}^t\theta & \cos^2 {}^t\theta & \sin {}^t\theta \cos {}^t\theta \\
 -\sin {}^t\theta \cos {}^t\theta & -\sin^2 {}^t\theta & \sin {}^t\theta \cos {}^t\theta & \sin^2 {}^t\theta
 \end{array} \right] \\
 &+ \frac{{}^tN}{{}^0\ell + \Delta^t\ell} \left[\begin{array}{cccc}
 1 & 0 & -1 & 0 \\
 0 & 1 & 0 & -1 \\
 -1 & 0 & 1 & 0 \\
 0 & -1 & 0 & 1
 \end{array} \right]
 \end{aligned}$$

with

$$\begin{aligned}
 {}^t\mathbf{k}_L &= \frac{EA}{{}^0\ell + \Delta^t\ell} \begin{bmatrix} \cos^2 {}^t\theta & \sin {}^t\theta \cos {}^t\theta & -\cos^2 {}^t\theta & -\sin {}^t\theta \cos {}^t\theta \\ \sin {}^t\theta \cos {}^t\theta & \sin^2 {}^t\theta & -\sin {}^t\theta \cos {}^t\theta & -\sin^2 {}^t\theta \\ -\cos^2 {}^t\theta & -\sin {}^t\theta \cos {}^t\theta & \cos^2 {}^t\theta & \sin {}^t\theta \cos {}^t\theta \\ -\sin {}^t\theta \cos {}^t\theta & -\sin^2 {}^t\theta & \sin {}^t\theta \cos {}^t\theta & \sin^2 {}^t\theta \end{bmatrix} \\
 {}^t\mathbf{k}_{NL} &= \frac{{}^tN}{{}^0\ell + \Delta^t\ell} \begin{bmatrix} 1 & 0 & -1 & 0 \\ 0 & 1 & 0 & -1 \\ -1 & 0 & 1 & 0 \\ 0 & -1 & 0 & 1 \end{bmatrix}. \tag{8.26}
 \end{aligned}$$

Comparing ${}^t\mathbf{k}_L$ with the stiffness matrix of the linear truss element given in equation (2.33), we can see that ${}^t\mathbf{k}_L$ corresponds to the stiffness matrix of a linear truss element which is geometrically identical to the nonlinear truss element at time t . Therefore, the interpretation of ${}^t\mathbf{k}_L$ – the linear part of the tangent stiffness matrix – is that it corresponds to a linear stiffness matrix which incorporates the change of geometry of the element due to the deformations.

The matrix ${}^t\mathbf{k}_{NL}$ – the nonlinear part of the tangent stiffness matrix – gives the stiffness contribution due to the force tN in the element.

Since we assumed that the strains are small we can generally set ${}^0\ell + \Delta^t\ell = {}^0\ell$ in (8.26).

Example 8.3

Interpret the coefficients of the truss nonlinear stiffness matrix (8.26) imposing unit end displacements.

Solution

For convenience, suppose that the truss element is horizontal at time t , as shown in Figure 8.13a. In Figure 8.13b, we show the unit end displacement

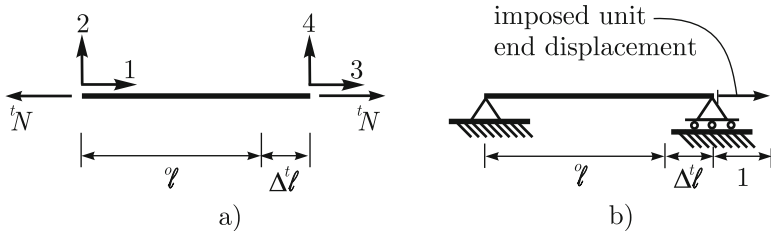


Fig. 8.13. a) Horizontal truss element at time t ; b) Unit end displacement imposed

of magnitude 1 which is imposed at the local degree of freedom 3 while the

remaining degrees of freedom are fixed. The axial force acting on the bar after the imposition of the unit end-displacement is given by

$$\frac{EA}{0\ell} (\Delta^t \ell + 1) = \frac{EA}{0\ell} \Delta^t \ell + \frac{EA}{0\ell} = {}^t N + \frac{EA}{0\ell}.$$

Since ${}^t N$ was already acting on the bar at time t , the force necessary to introduce the unit end displacement is

$${}^t k_{33} = \frac{EA}{0\ell}.$$

Let us verify that this is the ${}^t k_{33}$ which is obtained from (8.26). Considering that ${}^t \theta = 0$, (8.26) gives

$${}^t k_{33} = {}^t k_{L33} + {}^t k_{NL33} = \frac{EA}{0\ell + \Delta^t \ell} + \frac{{}^t N}{0\ell + \Delta^t \ell}. \quad (8.27)$$

Introducing the relation ${}^t N = \frac{EA}{0\ell} \Delta^t \ell$ into (8.27), we obtain

$${}^t k_{33} = \frac{EA}{0\ell + \Delta^t \ell} + \frac{EA \Delta^t \ell}{0\ell (0\ell + \Delta^t \ell)} = \frac{EA}{0\ell + \Delta^t \ell} \left(1 + \frac{\Delta^t \ell}{0\ell} \right) = \frac{EA}{0\ell}. \quad (8.28)$$

Note that from equilibrium

$${}^t k_{31} = -\frac{EA}{0\ell}, \quad {}^t k_{32} = 0 \quad \text{and} \quad {}^t k_{34} = 0$$

which can be easily obtained from (8.26).

Now consider the unit end displacement imposed for the local degree of freedom 4 as shown in Figures 8.14a and 8.14b. The forces required to guarantee equilibrium after the introduction of the unit end displacement lead to

$${}^t k_{14} = 0, \quad {}^t k_{24} = -\frac{{}^t N}{0\ell + \Delta^t \ell}, \quad {}^t k_{34} = 0 \quad \text{and} \quad {}^t k_{44} = \frac{{}^t N}{0\ell + \Delta^t \ell}.$$

Note that ${}^t k_{14} = {}^t k_{34} = 0$ and that the stiffness coefficients above are those of ${}^t \mathbf{k}_{NL}$, see (8.26). □

Example 8.4

Consider that the truss structure of Figure 8.15a is subjected to the imposed horizontal displacement that leads to the configuration at time t as shown in Figure 8.15b. Evaluate the tangent stiffness associated with the vertical displacement δ .

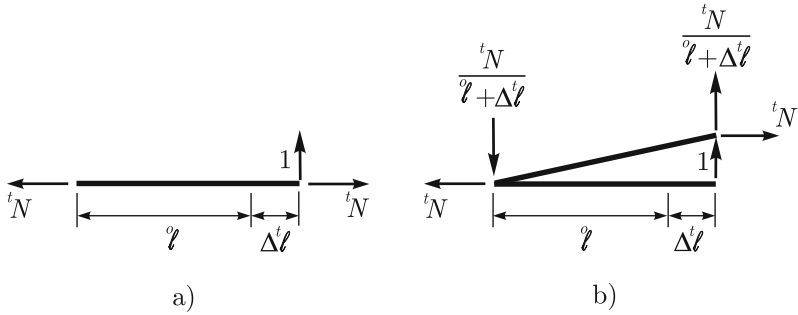


Fig. 8.14. a) Horizontal truss element at time t ; b) Equilibrium considering the unit end transverse displacement

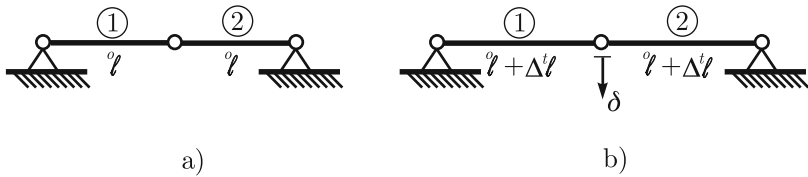


Fig. 8.15. a) Configuration at time 0; b) Configuration at time t

Solution

We can directly obtain the stiffness from the truss bar stiffness matrix derived above,

$$\begin{aligned}
 {}^t k &= {}^t k_{44}^{(1)} + {}^t k_{22}^{(2)} = {}^t k_{NL44} + {}^t k_{NL22} \\
 &= \frac{{}^t N}{l + \Delta l} + \frac{{}^t N}{l + \Delta l} = \frac{2 {}^t N}{l + \Delta l}.
 \end{aligned}$$

We note that ${}^t k$ is only due to ${}^t k_{NL}$ since the bars in the configuration at time t are still horizontal, and that the stiffness is proportional to the axial force in the bars.

□

8.3 Determination of ultimate loads leading to structural collapse

Considering a spatial load distribution acting on a structure, it is of great interest to calculate the value of the load multiplier that causes the structure to lose its capability of sustaining a further increase in load, *i.e.*, which causes the structural collapse.

Structural collapse is a very involved subject and our objective in this section is to only discuss briefly some basic facts.

In Section 8.1 we have already encountered situations in which the structure lost its ability to sustain a further increase in load, namely Examples 8.1 and 8.2.

We examine, through the following example, another situation of interest. □

Example 8.5

Consider the structure shown in Figure 8.16a, where k is a rotational spring. The bar is assumed to be rigid. Find the equilibrium configurations when tR is increased.

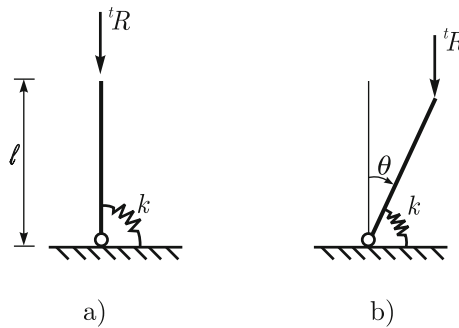


Fig. 8.16. a) Initial configuration; b) Potential deformed configuration

Solution

Let us examine possible equilibrium configurations. The bar remaining vertical gives a configuration which is always possible and, of course, in such a case the axial force in the bar is

$${}^tN = -{}^tR.$$

Consider the equilibrium configuration shown in Figure 8.16b. Moment equilibrium requires

$$-{}^tR\ell \sin \theta + M_k = 0$$

where M_k is the moment associated with the rotational spring which is given by

$$M_k = k\theta$$

leading to

$$- {}^tR\ell \sin \theta + k\theta = 0$$

which is satisfied by the undeformed configuration ($\theta = 0$) and by the configuration which corresponds to

$${}^tR = \frac{k\theta}{\ell \sin \theta}.$$

Since

$$\frac{\theta}{\sin \theta} > 1 \text{ for } \theta \neq 0$$

an equilibrium configuration with $\theta \neq 0$ is only possible for

$${}^tR > \frac{k}{\ell}.$$

The equilibrium configurations which are possible are summarized in Figure 8.17a: Up to the load ${}^tR = \frac{k}{\ell}$ there is only one equilibrium configuration possible and it corresponds to the vertical position of the bar. At the load ${}^tR = \frac{k}{\ell}$ there is a branching of the equilibrium paths, which is known as a bifurcation. For load levels greater than the bifurcation load, there are three possible equilibrium configurations as schematically shown in Figure 8.17a by B , B' and B'' .

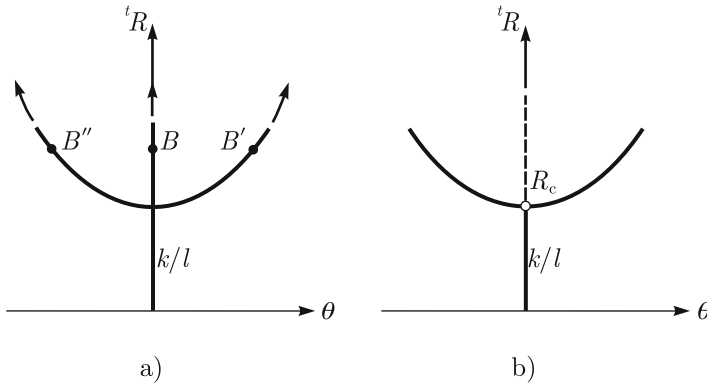


Fig. 8.17. a) Possible equilibrium configurations; b) Possible equilibrium configurations and their stability: the solid line represents stable equilibrium configurations while the dashed line unstable equilibrium configurations

Now consider that we increase the load “slowly” from zero to a load greater than the bifurcation or critical load $R_c = \frac{k}{\ell}$. We may then ask which equilibrium path will be followed and this question prompts the discussion below. □

Stability of an equilibrium configuration

The basic idea associated with the concept of an equilibrium configuration being stable is that if we introduce a small perturbation, for example through any small imposed force acting during a short period of time, the resulting motion will remain close to the equilibrium configuration, just like in linear analysis. Of course, there are many rigorous definitions of stability and formulations to verify whether an equilibrium configuration of a system/structure is stable or not (see *e.g.* Thompson and Hunt, 1973). Since our objective here is only to discuss the subject in an introductory and conceptual manner, we adopt the above concept and verify – in our small example above – the stability of the equilibrium state by identifying if the total potential energy (see Section 5.3) is at a local minimum for the configuration. That is, we use the result that for a conservative system an equilibrium configuration is stable if the total potential energy is at a local minimum³.

Let us examine the stability of the equilibrium configurations for the problem described in Figure 8.16. Since the bar is rigid, the strain energy is given by

$$U(\theta) = \frac{1}{2}k\theta^2$$

and, therefore, the total potential energy is given by

$$\Pi(\theta, {}^tR) = \frac{1}{2}k\theta^2 - {}^tR\ell(1 - \cos\theta).$$

Verifying the stability as defined above, we have that for $0 < {}^tR < R_{cr}$ the equilibrium configurations are stable. For ${}^tR > R_{cr}$ and $\theta = 0$ the equilibrium configurations are unstable and for $\theta \neq 0$ they are stable. The configuration that defines the bifurcation is itself unstable.

In Figure 8.17b we redraw Figure 8.17a using the solid lines to represent stable configurations and the dashed line to represent those which are unstable. Based on these conclusions, if we increase tR from zero, very slowly, the “deformed” configuration corresponds to $\theta = 0$ for ${}^tR < R_{cr}$. For a given ${}^tR > R_{cr}$ we could theoretically have a deformed configuration corresponding to $\theta > 0$, $\theta = 0$ or $\theta < 0$. However, any perturbation would lead to a configuration corresponding to either $\theta > 0$ or $\theta < 0$.

The bifurcation phenomenon is also referred to as buckling due to the fact that, conceptually, it is the same kind of instability that causes a straight column subjected to a compressive load to adopt an alternative curved, *i.e.* buckled, equilibrium configuration, when the magnitude of the load reaches a certain value, *i.e.*, the critical or buckling load.

We summarize in Table 8.1 the basic stability behaviors of 1-D structural systems. Problem 1 is equivalent to that of Example 8.1 since the spring is

³ We refer the reader to the Lagrange-Dirichlet theorem which establishes rigorously a sufficient condition for the stability of an equilibrium configuration

equivalent to the truss element with $k = \frac{EA}{\ell}$. In the response of the systems, we have identified in Table 8.1 the stability status of the equilibrium configurations using the same convention as adopted for Figure 8.17b. The point for which the system changes its stability is called a *singular* or *critical point* and the associated load is the *critical load*. These points are identified for all problems described in Table 8.1. The critical point of Problem 1 is defined as a *limit point*.

The limit point is a critical point for which there is no bifurcation of the equilibrium paths and for which there is no equilibrium configuration in its neighborhood for a load greater than the load associated with the limit point.

For Problems 2 to 4 the critical points are bifurcation points since we can clearly identify the branching of the equilibrium paths. They receive specific names, as shown in Table 8.1, that are connected to the characteristics of the post-critical (post-buckling) equilibrium paths. It can be shown that, for example, for Problem 3, if the load is increased very slowly from zero to the critical load and slightly beyond with a tiny horizontal load as a perturbation, a dynamic response initiates. Of course, the objective of presenting the problems in Table 8.1 is to give the reader insight into classical stability behaviors which serve as reference behaviors for more complex models.

The response of the systems summarized in Table 8.1 are for the *perfect system*, *i.e.*, with no imperfection in geometry or load application. Since no real structure or system to be modeled is totally free from imperfections, the response of the *imperfect system* is of interest. This, in particular, because the behavior may drastically change when we go from the perfect to the imperfect system, as discussed below.

In Table 8.2 we show the response of the problems of Table 8.1 when geometrical imperfections are considered. For Problem 1, although there is a change in the magnitude of the critical load, the qualitative behavior remains the same. For Problem 2, there is a change in the qualitative behavior of the system, that is, the system no longer displays a bifurcation point. The same happens for Problem 3. However, for this case, the response of the imperfect system has a limit point, instead of the bifurcation, with a critical load magnitude lower than that of the perfect system. Note that depending on the magnitude of the imperfection, the critical load may be significantly lower than that of the perfect system. For Problem 4, depending on the sense of the imperfection the system behaves either as 2 or 3. We observe that when the imperfection leads to a sharp decrease in the critical load, the structure is said to be sensitive to imperfections.

An important conclusion reached by studying the behavior of the imperfect systems is that the response may qualitatively change. Most importantly, however, is that the critical load may be significantly lower leading to collapse much earlier than predicted for the perfect system.

Table 8.1. Stability behavior of selected models

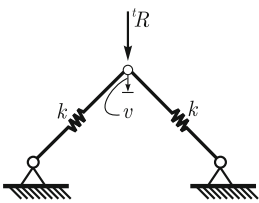
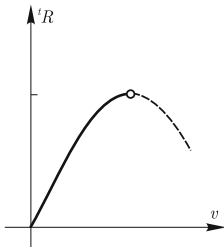
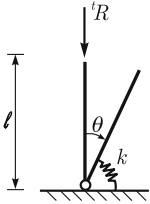
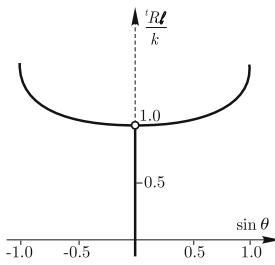
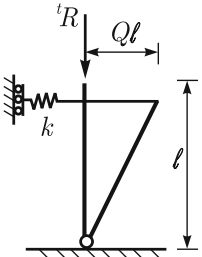
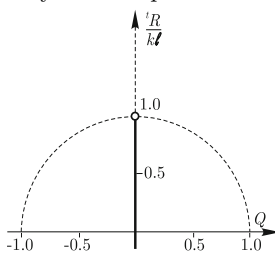
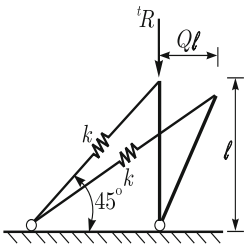
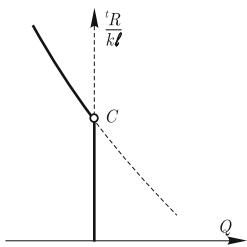
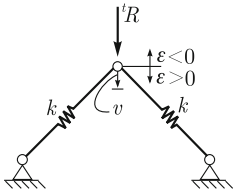
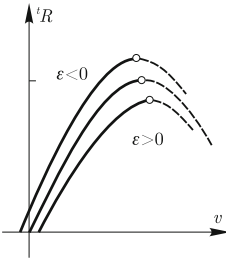
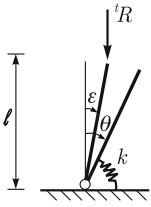
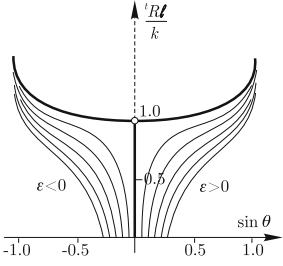
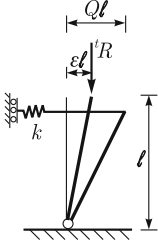
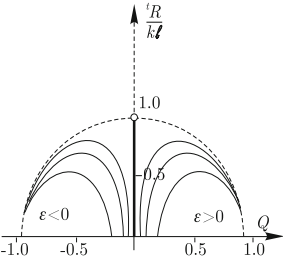
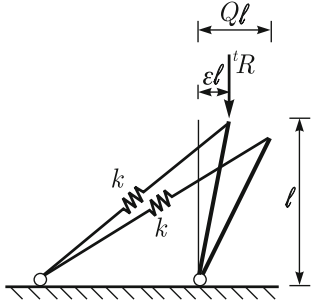
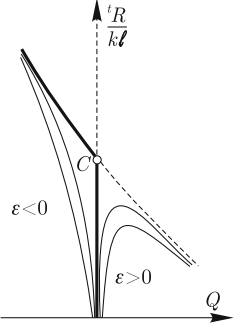
Problem	Perfect system
<p>1)</p> 	<p>Limit point</p> 
<p>2)</p> 	<p>Stable symmetric point of bifurcation</p> 
<p>3)</p> 	<p>Unstable symmetric point of bifurcation</p> 
<p>4)</p> 	<p>Asymmetric point of bifurcation</p> 

Table 8.2. Behavior of selected models subjected to geometrical imperfections. The horizontal axes of displacements include the imperfections

Problem	System with imperfection
<p>1)</p>  <p>A truss structure with two bars of stiffness k meeting at a top joint. A vertical load R is applied downwards. The top joint is displaced vertically by v. Imperfections $\epsilon < 0$ and $\epsilon > 0$ are shown as vertical offsets from the vertical axis.</p>	<p>Limit point</p>  <p>A graph showing the load R versus displacement v. The curves show a peak (limit point) followed by a softening region. Imperfections $\epsilon < 0$ and $\epsilon > 0$ shift the peak and the subsequent softening behavior.</p>
<p>2)</p>  <p>A vertical bar of length l and stiffness k is fixed at the bottom. A horizontal load R is applied at the top, causing a deflection θ. An imperfection ϵ is shown as a small horizontal offset at the top.</p>	<p>Stable symmetric point of bifurcation</p>  <p>A graph showing the load R/k versus $\sin \theta$. The curves exhibit a stable symmetric point of bifurcation at $R/k = 1.0$. Imperfections $\epsilon < 0$ and $\epsilon > 0$ shift the bifurcation point.</p>
<p>3)</p>  <p>A vertical bar of length l and stiffness k is fixed at the bottom. A horizontal load R is applied at the top, causing a deflection Ql. An imperfection ϵl is shown as a small horizontal offset at the top.</p>	<p>Unstable symmetric point of bifurcation</p>  <p>A graph showing the load $R/k l$ versus Q. The curves exhibit an unstable symmetric point of bifurcation at $R/k l = 1.0$. Imperfections $\epsilon < 0$ and $\epsilon > 0$ shift the bifurcation point.</p>
<p>4)</p>  <p>A vertical bar of length l and stiffness k is fixed at the bottom. A horizontal load R is applied at the top, causing a deflection Ql. An imperfection ϵl is shown as a small horizontal offset at the top.</p>	<p>Asymmetric point of bifurcation</p>  <p>A graph showing the load $R/k l$ versus Q. The curves exhibit an asymmetric point of bifurcation at $R/k l = 1.0$. Imperfections $\epsilon < 0$ and $\epsilon > 0$ shift the bifurcation point.</p>

Now let us consider the Problem 3 of Table 8.1, but for a flexible bar, *i.e.*, a truss bar. The problem is summarized in Figure 8.18 where we have placed the bar horizontally.

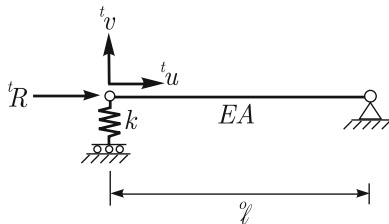


Fig. 8.18. Problem 3 of Table 8.1 with flexible bar

Considering the equilibrium configuration for a horizontal configuration of the bar, we can write

$$\begin{aligned} {}^tR &= -{}^tN \\ \Delta^t\ell &= \frac{{}^tN^0\ell}{EA} \\ {}^tu &= -\Delta^t\ell = -\frac{{}^tN^0\ell}{EA} = \frac{{}^tR^0\ell}{EA} \\ {}^tv &= 0. \end{aligned}$$

The tangent stiffness matrix is given by

$${}^t\mathbf{K} = \frac{EA}{{}^0\ell + \Delta^t\ell} \begin{bmatrix} 1 & 0 \\ 0 & 0 \end{bmatrix} + \frac{{}^tN}{{}^0\ell + \Delta^t\ell} \begin{bmatrix} 1 & 0 \\ 0 & 1 \end{bmatrix} + \begin{bmatrix} 0 & 0 \\ 0 & k \end{bmatrix}$$

where we have presented above the ${}^t\mathbf{k}_L$ and the ${}^t\mathbf{k}_{NL}$ matrices of the truss bar and the contribution of the spring. We can re-write the tangent stiffness matrix as

$${}^t\mathbf{K} = \begin{bmatrix} \frac{EA}{{}^0\ell} & 0 \\ 0 & k - \frac{{}^tR}{{}^0\ell + \Delta^t\ell} \end{bmatrix}.$$

The incremental displacements can be evaluated by solving

$${}^t\mathbf{K} \Delta\mathbf{u} = \Delta\mathbf{R} \tag{8.29}$$

where $\Delta\mathbf{R}^T = \begin{bmatrix} \Delta R & 0 \end{bmatrix}$. Therefore $\Delta\mathbf{u}^T = \begin{bmatrix} \Delta u & 0 \end{bmatrix}$ is a solution of (8.29) and if $\det {}^t\mathbf{K} \neq 0$ it is the unique solution. Note that

$$\det {}^t\mathbf{K} = \frac{EA}{{}^0\ell} \left(k - \frac{{}^tR}{{}^0\ell + \Delta{}^t\ell} \right)$$

where

$${}^tR = k({}^0\ell + \Delta{}^t\ell) = k{}^t\ell$$

leads to $\det {}^t\mathbf{K} = 0$ and characterizes a singular or critical point.

The simple idea presented above can be generalized for structures with many degrees of freedom. Let us assume that the load vector is defined by

$${}^t\mathbf{R} = {}^t\lambda\mathbf{R}_0$$

where \mathbf{R}_0 is a reference load vector and ${}^t\lambda$ is the load multiplier. In addition, suppose that we are using the incremental procedure to obtain the structural response. For a given time t , we seek the incremental displacements using

$${}^t\mathbf{K} \Delta\mathbf{U} = \Delta\lambda \mathbf{R}_0 \quad (8.30)$$

and as long as $\det {}^t\mathbf{K} \neq 0$ we can solve for $\Delta\mathbf{U}$. When ${}^t\mathbf{K}$ becomes singular, *i.e.*, $\det {}^t\mathbf{K} = 0$, we have reached a singular or critical point. Conceptually, we have an analogous situation to the 1-D problem. We may have either a bifurcation of the equilibrium path or a limit point. In the limit point case there is no branching of the equilibrium path and an equilibrium configuration in the vicinity of the critical point is associated with a decrease in ${}^t\lambda$. In this case it is still possible to obtain the post-critical response of the structure by means of an incremental solution. However, adequate procedures should be used since the (immediate) post-critical path is associated with a decrease in ${}^t\lambda$. There are incremental strategies which have as unknowns not only the incremental displacements $\Delta\mathbf{u}$ but also the increment $\Delta\lambda$ of the load multiplier parameter which may be negative, see Bathe, 1996.

In many cases of practical interest the critical point may be taken as the ultimate configuration at which the structure can no longer support a further increase of the external load. Therefore, in such cases the determination of the critical point and associated loading characterizes the ultimate load carrying capacity of the structure.

An incremental procedure always determines only one equilibrium path. Therefore, when a critical point is reached, to identify the nature of the critical point, the basic behaviors summarized in Tables 8.1 and 8.2 need be considered. For perfect systems, the nature of the critical point may indicate the kind of imperfection to be considered in the model in order to avoid an overestimation of the actual physical collapse load of the structure.

In the above approach, the determination of a critical point requires that the incremental solution be undertaken up to the critical point. Sometimes it is convenient to have an estimate of the critical load without performing the full incremental solution. We describe such approach below.

Linearized buckling analysis

The basic assumption of a linearized buckling analysis is that the tangent stiffness matrix varies linearly with respect to the load parameter λ as

$${}^{\tau}\mathbf{K} = {}^{t-\Delta t}\mathbf{K} + \lambda \left({}^t\mathbf{K} - {}^{t-\Delta t}\mathbf{K} \right) \quad (8.31)$$

where τ is the time associated with

$${}^{\tau}\mathbf{R} = {}^{t-\Delta t}\mathbf{R} + \lambda \left({}^t\mathbf{R} - {}^{t-\Delta t}\mathbf{R} \right). \quad (8.32)$$

We are interested in determining the value of λ which makes ${}^{\tau}\mathbf{K}$ singular, *i.e.*,

$$\det {}^{\tau}\mathbf{K} = 0 \quad (8.33)$$

or equivalently

$${}^{\tau}\mathbf{K}\phi = \mathbf{0} \quad (8.34)$$

with $\phi \neq \mathbf{0}$. The values of λ_i that satisfy (8.33) or (8.34) can be found by solving an eigenvalue problem as detailed in Bathe, 1996 which also gives ϕ_i as the eigenvectors.

The eigenvalues λ_i define through equation (8.32) the buckling loads and the associated eigenvectors define the buckling modes, since by equation (8.34) we can see that a buckling mode corresponds to a valid displacement solution associated with no increment in the load.

The quality of the predictions obtained with the linearized buckling analysis depends primarily on whether the approximation adopted for the tangent stiffness matrix given by (8.31) is sufficiently accurate.

In general, we take ${}^{t-\Delta t}\mathbf{K} = {}^0\mathbf{K}$, *i.e.*, the stiffness matrix prior to the application of external loads. When the magnitude of the displacements which take place prior to the critical point is small, the assumption implicitly contained in (8.31) is adequate. Then, the linearized buckling analysis is quite useful.

Finally, we note that the buckling modes may be used to generate imperfections. When properly scaled, buckling modes can be added to the initial geometry of the structure generating an imperfect initial geometry, which may correspond to a significantly lower critical load than that of the perfect structure. An example of this procedure can be found in Bathe, 1996.

8.4 Modeling nonlinear problems

As mentioned at the beginning of this chapter, the finite element nonlinear formulations of the mathematical models of Chapters 3 and 4 are out of the

scope of this book and we refer the reader to Bathe, 1996 where such formulations are given. We note, however, that the nonlinear formulation presented for the truss element is a valuable aid for conceptually understanding the nonlinear finite element matrices of more complex formulations. In fact, we note that there are analogies between the nonlinear formulation of the truss element and that of every finite element presented in Chapter 6. Namely:

- The incremental formulation is the same as that presented in Section 8.2.
- For each element the tangent stiffness matrix can be decomposed into a ${}^t\mathbf{k}_L$ and a ${}^t\mathbf{k}_{NL}$ with analogous interpretations as for the truss element, *i.e.*, ${}^t\mathbf{k}_L$ accounts for the additional straining of the element and ${}^t\mathbf{k}_{NL}$ for the effect that there are already internal forces/stresses in the element.

However, there are many complex additional considerations when considering nonlinear 2-D, 3-D, beam and shell analyses, and these are particularly complex because the details of the formulations matter a great deal in order to obtain reliable, accurate and effective solutions, see Bathe, 1996.